DEUTSCHES ELEKTRONEN-SYNCHROTRON DESY

DESY 82-050
August 1982

A REVIEW OF TWO PHOTON PHYSICS

by

Susan Cooper

NOTKESTRASSE 85 · 2 HAMBURG 52

To be sure that your preprints are promptly included in the
HIGH ENERGY PHYSICS INDEX ,
send them to the following address (if possible by air mail) :

DESY
Bibliothek
Notkestrasse 85
2 Hamburg 52
Germany

DESY 82-050
August 1982

A REVIEW OF TWO PHOTON PHYSICS

Invited talk given at 2nd International Conference
on Physics in Collision, Stockholm, 2-4 June 1982

by

SUSAN COOPER

Deutsches Elektronen-Sychrotron DESY,
Hamburg, Germany

This talk is intended as an introduction for those not yet expert in two-photon physics, especially those e^+e^- one-photon physicists who still think of two-photon events as background. I will concentrate on the physics questions involved, especially emphasizing the areas where I feel progress can be made in the near future, and of necessity leaving most experimental details to be found in the references. After a quick survey of the field and a few words about kinematics, I will discuss in detail two major fields: the photon structure function and resonance production.

INTRODUCTION

What is <u>two photon</u> physics ?

Our subject is the collisions of two phctons. The first problem is clearly to obtain two photon beams to collide with one another. Fortunately electron beams emit many bremsstrahlung photons, meaning that e^+e^- colliding beam machines are also colliding photon machines. The properties of our photon beams are those of bremsstrahlung: low energy and small angle relative to the electron beams, and high intensity.

Photons emitted at small angles are almost real, unlike the far-off-mass-shell photon created in e^+e^- annihilation. The annihilation process decreases as $1/s$ ($s=(2E_{beam})^2$) due to the presence of the photon mass ($m^2=s$) in the photon propagator. In the two-photon process this suppression is absent because the photon mass can remain small as the electron beam energy increases. As a result, the two-photon cross section increases logarithmically with s, overtaking the one-photon cross section at beam energies of a few GeV. Although the detection efficiency for two-photon events is relatively small (~10%), at PEP/PETRA energies the typical detector has approximately equal numbers of one- and two-photon

events. This means that we now have large numbers of events available to do physics with!

Despite early worries to the contrary, it has proven fairly easy to separate one- and two-photon events at PEP/PETRA beam energies. Two-photon events are characterized by low visible energy, since the electron and positron, which carry away most of the available energy, are usually scattered at angles too small to be detected. A requirement that the visible energy be less than the electron beam energy removes almost all annihilation events. Annihilation events with a very hard bremsstrahlung in the initial state will remain, but are characterized by having all the missing energy on one side, i.e. the missing momentum is in the beam direction and is in magnitude approximately equal to the missing energy. Two photon events are not restricted in this way, since the electron and positron carry off energy and momentum in both directions. The small scattering angles also mean that the products of the $\gamma\gamma$ collision have low net transverse momentum p_t to the e^+e^- beam directions. This allows selection of exclusive events $\gamma\gamma \to X$ from events where some particles are undetected due to incomplete solid angle or lack of neutral particle detection. These kinematic characteristics have proven successful in obtaining clean samples of two-photon events without requiring the detection (tag) of the scattered electron and/or positron[1].

What is two photon physics ?

With our two colliding, almost-real photons we have the inverse of decay processes like $\pi^0 \to \gamma\gamma$. Measurement of the coupling of a resonance to two photons can provide a test of its assignment to a $q\bar{q}$ nonet: a large deviation from the expected value might indicate that the resonance is not $q\bar{q}$, but something more exotic such as a four-quark or gluonium state. In addition, the cleaner two-photon channel might be able to illuminate some questionable resonances which have remained illusive in hadronic reactions. Resonance production will be discussed in detail in the last section of this talk.

Of course, two photons don't always produce resonances. There is also a continuum, much of which can be attributed to the Vector Dominance Model (VDM) process where the two photons become ρ^0's before they collide, and thus interact as hadrons. Measurement of the total cross section $\gamma\gamma \to X$ as a function of the $\gamma\gamma$ invariant mass $W_{\gamma\gamma}$ turns out to be very difficult due to the low acceptance (remember hadron-hadron scattering is peaked along the beam direction) and the resulting dependence on a Monte Carlo model to correct for the undetected particles. Early measurements[2] are in only rough agreement with each

other and with the VDM prediction. However, subsequent studies[3] have shown that the permissible range of the Monte Carlo model parameters is even larger than thought at that time. The systematic errors are thus very large. A better measurement of the total cross section requires better acceptance for both charged and neutral particles, especially in the forward direction, to reduce the dependence on a Monte Carlo model.

At large momentum transverse to the beam, the contribution from the hadron-like VDM process is small and the reaction $\gamma\gamma \to q\bar{q}$ is expected to dominate, as shown in Figure 1. The cross section for $\gamma\gamma \to q\bar{q}$ is related to that for $\gamma\gamma \to \mu^+\mu^-$ by the factor $R_{\gamma\gamma}=3\sum(\text{quark charge})^4=34/27$ for fractionally charged quarks[4]. One observes $\gamma\gamma \to q\bar{q}$ as two hadron jets. The inclusive p_t distribution for hadrons coming from $\gamma\gamma \to q\bar{q}$ is expected[5] to fall asymptotically as p_t^{-4}, whereas hadrons coming from the VDM process would show the much steeper fall-off typical of hadronic processes in this energy range. Currently available results[6] for the inclusive p_t^2 spectrum show a high-p_t tail above 2 GeV^2 which is consistent with p_t^{-4}, as shown in Figure 2. When the hadrons are grouped into jets, the cross section as a function of the p_t^2 of the jets is as shown in Figure 3. The data lie above the expectation for $\gamma\gamma \to q\bar{q}$ at $p_t^2 = 5$ GeV^2, and fall nearer for higher p_t^2's, becoming consistent with the expected value by $p_t^2 = 10$ GeV^2 where, however, the statistical errors are very large. These results are based on an integrated luminosity of 9000nb^{-1}, so we can expect an appreciable improvement when the presently available 60000nb^{-1} at PETRA and 40000nb^{-1} at PEP are used.

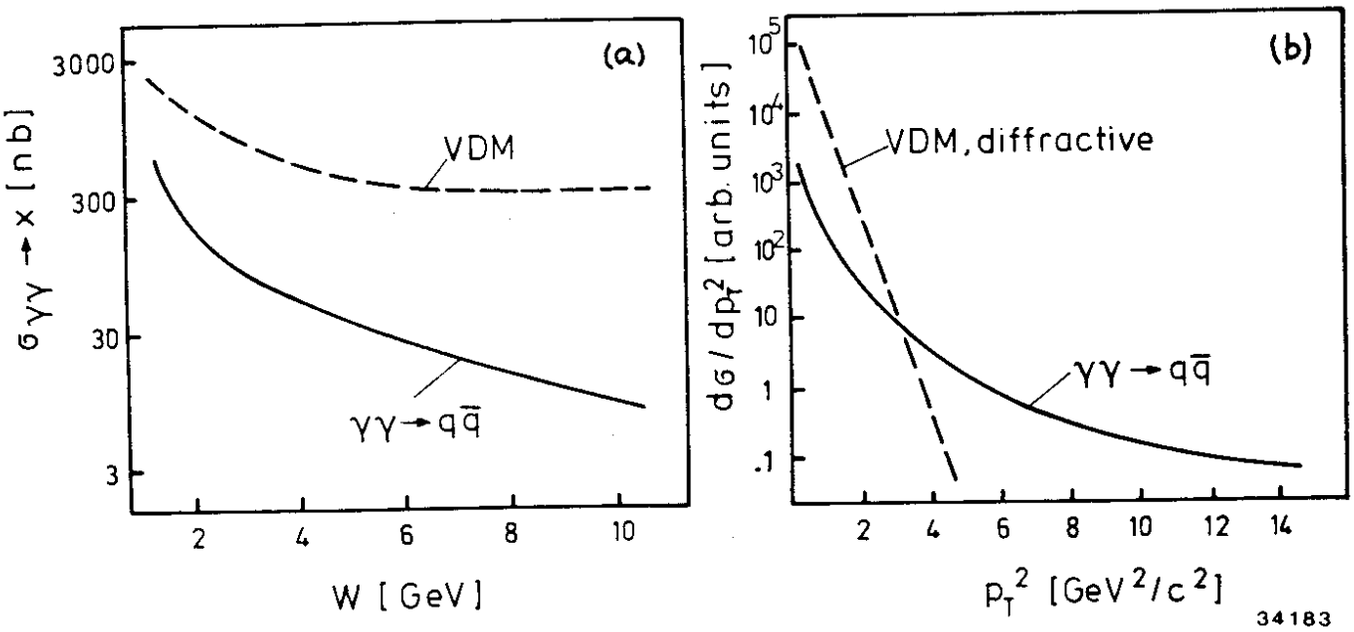

Figure 1. Approximate cross sections for $\gamma\gamma \to \rho^0\rho^0 \to X$ and $\gamma\gamma \to q\bar{q} \to X$ (a) as a function of $W_{\gamma\gamma}$, the total c.m. energy of the $\gamma\gamma$ system, and (b) as a function of p_t^2 of the individual hadrons.

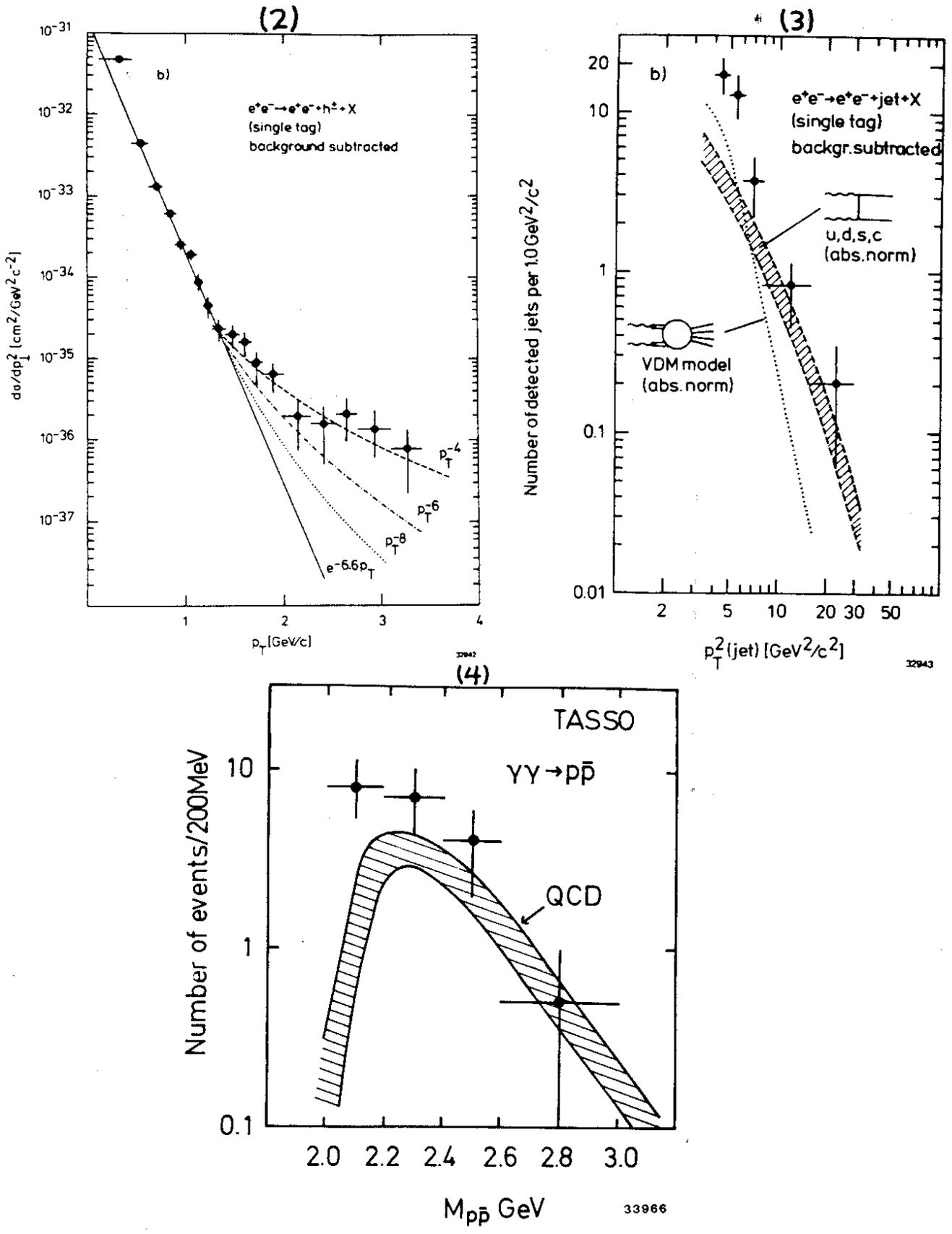

Figure 2. TASSO inclusive hadron p_t spectrum for two-photon events.
Figure 3. TASSO jet p_t spectrum for two-photon events, compared to expectations for VDM and $\gamma\gamma \to q\bar{q}$ models.
Figure 4. Preliminary TASSO observed rate for $\gamma\gamma \to p\bar{p}$ compared to QCD calculation (hatched area).

Production of meson or baryon pairs ($\gamma\gamma \to M\bar{M}$ or $\gamma\gamma \to B\bar{B}$) at large transverse momentum is calculable[7] in QCD. Again, early results[8] (Figure 4) are encouraging, and more events at higher p_t's are eagerly awaited. Because of questions asked at the conference, I have somewhat expanded this section on high-p_t phenomena over what I had time for at the conference. I regret that further discussion of this interesting field was not possible.

Another kinematic region where $\gamma\gamma \to q\bar{q}$ dominates over VDM and where comparisons to QCD can be made is when one of the photons is highly virtual. This occurs on those rare occasions when one of the electrons is scattered at large angle. This process, refered to as the high-Q^2 region or as deep inelastic electron-photon scattering, can be formulated in a way analogous to deep inelastic electron-nucleon scattering.

After an introduction to the kinematics of $\gamma\gamma$ scattering, I will discuss in detail the high-Q^2 region and then resonance production.

KINEMATICS

We observe $\gamma\gamma \to X$ at e^+e^- storage rings as a subprocess of $e^+e^- \to e^+e^-X$, as shown in Figure 5. The incoming positron and electron both have energy E and 4-momenta p_1 and p_2 respectively. After scattering they have energies E_1' and E_2' and polar angles with respect to their original direction ϑ_1 and ϑ_2. The emitted photons have 4-momenta q_1, q_2 and energies $E_{\gamma 1}$, $E_{\gamma 2}$, and

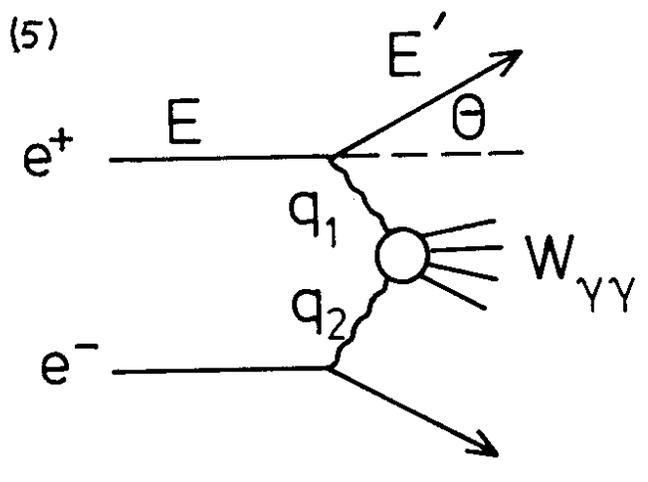

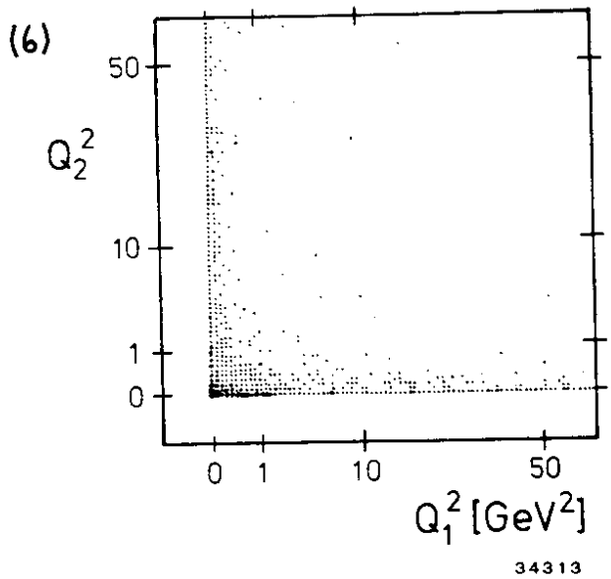

Figure 5. Diagram for $e^+e^- \to e^+e^-\gamma\gamma \to e^+e^-X$.
Figure 6. Photon-photon luminosity function for transverse photons as a function of the Q^2's of the two photons. The thickness of the points is proportional to the luminosity.

combine to form the system X of mass $W_{\gamma\gamma}=|q_1+q_2|$. The squares of the photon masses (q_1^2,q_2^2) are negative, and it is conventional to use instead

$$Q^2 = - q^2 = 4 E E' \sin^2(\vartheta/2) \approx E E' \vartheta^2$$

Virtual photons, with $Q^2\neq 0$, can have helicities $\lambda=\pm 1,0$. The longitudinal component ($\lambda=0$) vanishes as $Q^2\to 0$, leaving only transverse components for real photons. In general the process $e^+e^-\to e^+e^-X$ can be written as

$$\sigma_{ee\to eeX} = \sum_h L^h(q_1,q_2)\ \sigma^h_{\gamma\gamma\to X}(W_{\gamma\gamma},q_1^2,q_2^2)$$

where L^h is the photon-photon "flux factor" or "luminosity function" and the index h indicates the combinations of photon helicities[9].

Since we can only measure cross sections in kinematic regions where we have substantial luminosity, it is important to consider what the luminosity function looks like. The luminosity function for transverse photons is shown as a function of Q_1^2 and Q_2^2 in Figure 6, where the thickness of the points is proportional to the luminosity function. The very black dot in the corner indicates that the greatest luminosity occurs when both photons have $Q^2\approx 0$. This is where most of the $\gamma\gamma$ events come from, and is the region where the cut $\left|\sum \vec{p}_t\right| \sim 0$ is valid. This is the region where resonance production has been studied. The region where both photons have large Q^2 may well contain interesting physics, but we won't see it because the luminosity is practically nonexistent there. However there is small but significant luminosity along the two axes, where one photon has $Q^2\approx 0$ and the other has large Q^2. This is refered to as the high-Q^2 region, where deep inelastic $e\gamma$ scattering is studied.

DEEP INELASTIC ELECTRON-PHOTON SCATTERING

Events with one high-Q^2 photon are selected by requiring the detection of a scattered beam electron or positron at large angle. This is illustrated in Figure 7 where a high-Q^2 event is sketched in a "typical" all-purpose detector. The hadronic system X is detected in the central detector, which usually has a drift chamber in a solenoidal magnetic field for measurement of charged particles, surrounded by an electro-magnetic shower counter for measurement of photon energies. The scattered positron is detected in the end-cap shower counters, which typically cover the polar angle range between 0.1 and 0.5 radians. At a beam energy of 15 GeV, this angular coverage gives a Q^2 range up to about 50 GeV^2. The electron, scattered at small angle, passes undetected down the beam pipe.

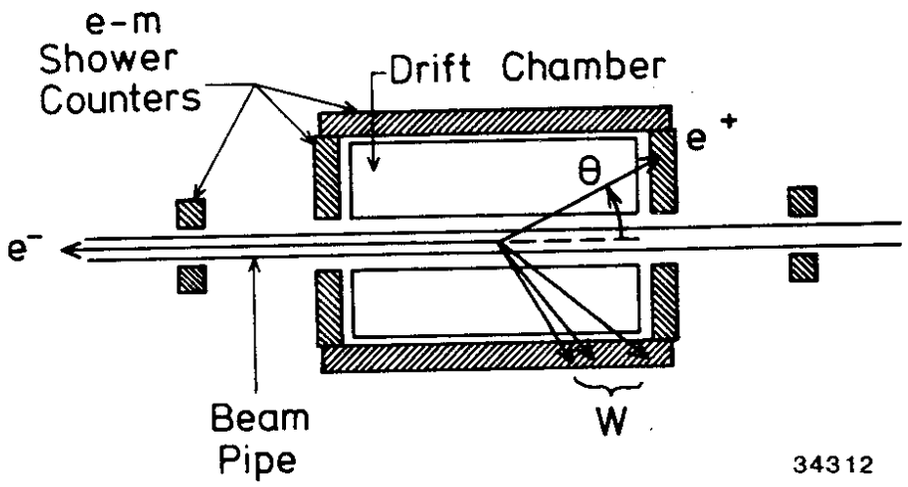

Figure 7. A high-Q^2 event in a typical detector.

The high-Q^2 photon has a longitudinal as well as transverse components, whereas the $Q^2 \approx 0$ photon is almost purely transverse. Thus the cross section will have two terms: σ^{TT} for both photons transverse and σ^{LT} for one longitudinal and one transverse (an interference term drops out when the azimuthal angles of the scattered electrons are integrated over)[10]:

$$\begin{aligned} \sigma_{ee\to eeX} &= L^{TT}\,\sigma^{TT} + L^{LT}\,\sigma^{LT} \\ &= L^{TT}\,(\,\sigma^{TT} + \varepsilon\,\sigma^{LT}\,) \end{aligned} \qquad (1)$$

This cross section can be re-written in terms of two photon structure functions F_1 and F_2 and the scaling variables x and y:

$$F_1 \equiv \frac{Q^2}{8\pi^2\alpha x}\,\sigma^{TT}\,, \qquad F_2 \equiv \frac{Q^2}{4\pi^2\alpha}\,(\,\sigma^{TT} + \sigma^{LT}\,)$$

$$x \equiv \frac{Q^2}{Q^2 + W^2}\,, \qquad y \equiv \frac{q_1 \cdot q_2}{p_1 \cdot q_2} \approx \frac{E_\gamma}{E}$$

$$\frac{d\,\sigma_{ee\to eeX}}{dx\,dQ^2\,dE_{\gamma 2}} = \frac{4\pi\alpha^2}{Q^4 x}\left\{\,(1-y)\,F_2(x,Q^2) + xy^2\,F_1(x,Q^2)\,\right\}N(E_{\gamma 2}) \qquad (2)$$

where $N(E_{\gamma 2})$ is the flux factor for the $Q^2 \approx 0$ photon. In regions where we have significant luminosity y is small, so that the term in F_1 may be neglected. This leaves us with one photon structure function F_2 to

measure as a function of x and Q^2. Note that this form is equivalent to (1), with the structure functions taking over the role of σ^{TT} and σ^{LT} and with L^{TT} replaced by the combination of $N(E_{\gamma 2})$ and the kinematic factors. Neglecting the F_1 term in (2) corresponds to setting $\varepsilon=1$ in (1).

The presence of structure functions in (2) suggests a comparison of $e^+e^-\rightarrow e^+e^-X$ with deep-inelastic electron-nucleon scattering, with in our case the nucleon target being replaced by a $Q^2\approx 0$ photon target. Electron-nucleon scattering as understood in the parton model is illustrated in Figure 8a. The incoming electron emits a high-Q^2 photon which sees the nucleon as a collection of quasi-free partons with small transverse momentum relative to the incoming electron direction. The photon is absorbed by one of the partons, knocking it out of the nucleon before it can interact with any of the other partons. This lack of interaction between the partons means that there is a fixed relation between the 4-momentum q of the photon, the 4-momentum P of the nucleon, and the fractional momentum x of the affected parton:

(8)

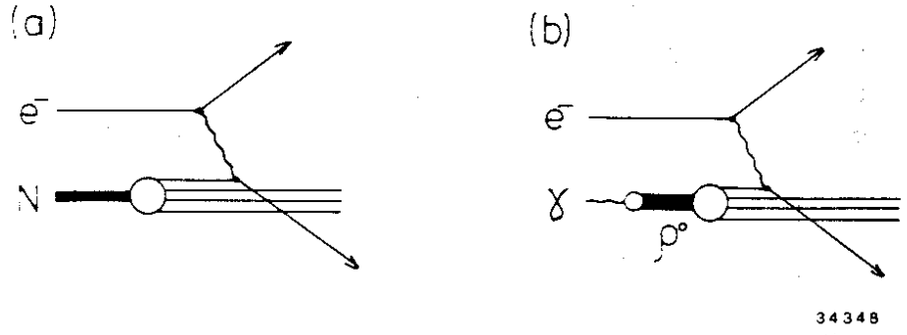

(9)

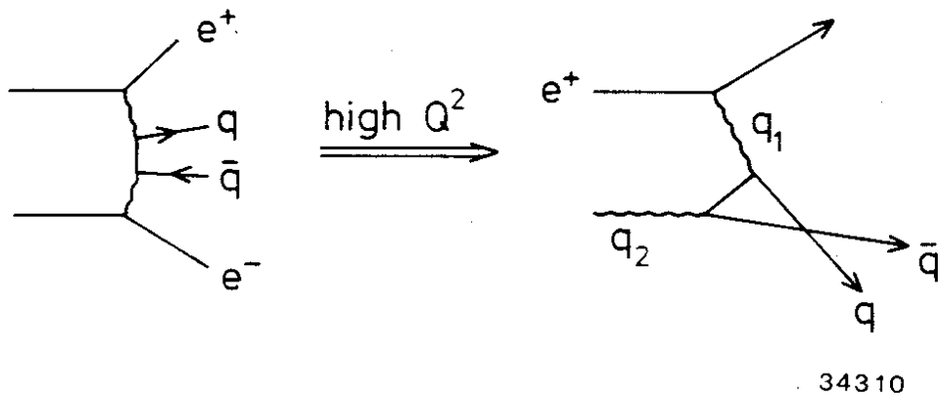

Figure 8. (a) $eN \rightarrow eX$ in the parton model; (b) $e\gamma \rightarrow eX$ for the ρ part of the photon.
Figure 9. $ee \rightarrow eeX$ and $e\gamma \rightarrow eX$ in the quark model.

$$x \equiv \frac{\text{longitudinal momentum of parton}}{\text{longitudinal momentum of nucleon}} = \frac{Q^2}{2\, q \cdot P}$$

In the case of $e\gamma \to eX$, the nucleon momentum P is replaced by the $Q^2 \approx 0$ photon momentum q_2, giving

$$x \equiv \frac{Q_1^2}{2\, q_1 \cdot q_2} = \frac{Q_1^2}{Q_1^2 + Q_2^2 + W^2} \approx \frac{Q^2}{Q^2 + W^2}$$

for $Q^2 \equiv Q_1^2$, $Q_2^2 \approx 0$ and $W = W_{\gamma\gamma}$= the mass of the system X. This is exactly the scaling variable x that we have defined previously.

There are two mechanisms which contribute to $e\gamma \to eX$. In the VDM picture (Figure 8b) the target photon is seen as a ρ meson which in turn has parton constituents, one of which absorbs the high-Q^2 photon. This contribution to F_2^γ behaves like F_2^N.

In the second mechanism which contributes to F_2^γ, the "parton constituents" of the photon target are the $q\bar{q}$ of our QED $\gamma\gamma \to q\bar{q}$ diagram, as shown in Figure 9. Unlike the constituents of a nucleon, they are not restricted to small transverse momenta, since they are not really constituents in the sense of being confined in a photon. Their transverse momentum spectrum continues to the kinematic boundary $p_t^{max} \approx W/2$. This additional freedom in p_t gives several important differences from the eN case:

a) x cannot always be interpreted as the ratio of the quark momentum to the photon momentum (only at $p_t \approx 0$),

b) the Callen-Gross relation $F_2 = 2xF_1$ does not hold (derivation uses $p_t \approx 0$)

c) F_2^γ even in lowest order does not show the scaling (independence of Q^2) that is true to lowest order in eN scattering, but rather grows with $\ln Q^2$.

The fact that the $q\bar{q}$ come from a photon, a fundamental particle of the theory, means that F_2^γ can be calculated, both in normalization and shape, whereas for F_2^N only the Q^2 evolution can be calculated. The calculation shows that F_2^γ increases with $\ln Q^2$ (whereas F_2^N decreases) and F_2^γ increases with x (F_2^N decreases). Both of these properties will make the $\gamma\gamma \to q\bar{q}$ part of F_2^γ easier to distinguish from higher twist ($1/Q^2$) or VDM ($\sim 1-x$) contributions than was the case for F_2^N.

Before describing these calculations, let us first consider how F_2^γ is to be measured and take a first look at the data. F_2^γ is a function of $Q^2 = 4\, E\, E' \sin^2(\vartheta/2)$, so we need to measure the scattered electron's energy and scattering angle, which is done in the endcap shower counter. F_2^γ is also a

function of $x = Q^2 / (Q^2 + W^2)$, so we also need to measure the total hadronic energy W. To really measure the total energy we would need to have a 100% efficient 4π detector for both charged and neutral particles. Lacking this, as we all are, we must

a) get as much of the energy as possible by building a new and better detector and/or work very hard to get as much as possible out of what we've got, and

b) use a model for the hadron formation in $e\gamma \rightarrow eX$ and a Monte Carlo detector simulation to relate $x_{meas} = Q^2 / (Q^2 + W_{meas}^2)$ to the real x.

To measure $F_2^\gamma(x,Q^2)$ we also need our efficiency as a function of x and Q^2, which we obtain using the same Monte Carlo simulation.

At present there are not enough statistics available to measure F_2^γ simultaneously as a function of x and Q^2, so each group has combined its data over its entire Q^2 range to measure the x dependence of F_2^γ. The PLUTO collaboration has shown[11] (Figure 11b) that their average Q^2 is roughly independent of x, providing some justification for this procedure.

For the actual measurement, a first approximation of F_2^γ is chosen. Monte Carlo events are generated with this F_2^γ and put through the

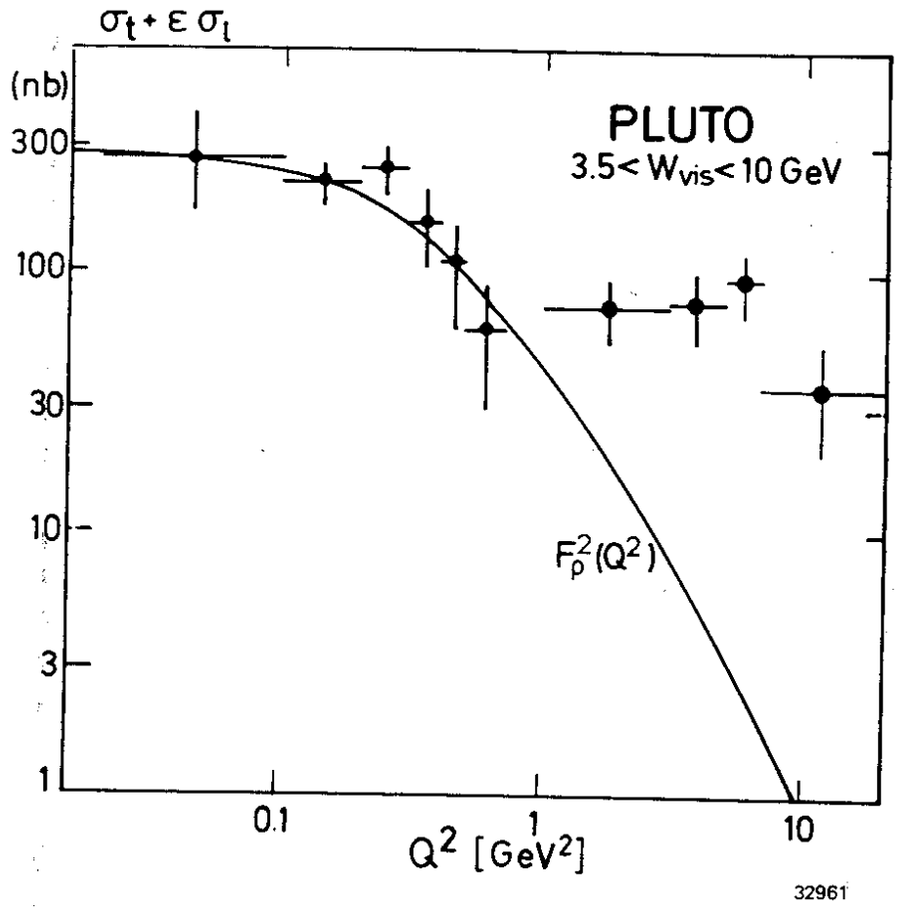

Figure 10. PLUTO total $\gamma\gamma$ cross section as a function of Q^2. The solid line shows the VDM prediction.

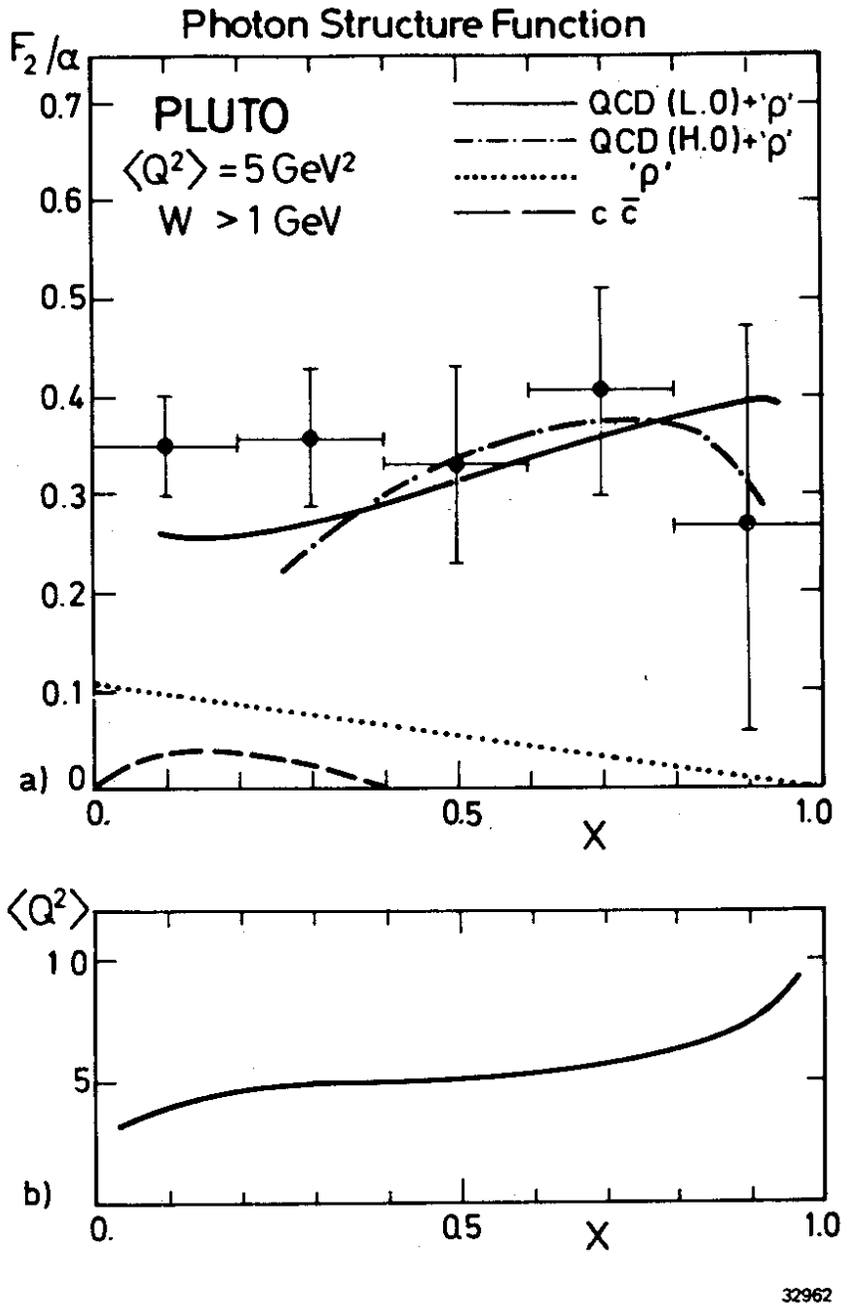

Figure 11. (a) PLUTO photon structure function averaged over $1 < Q^2 < 15$ GeV^2. Also shown are: the expected ρ structure function 'ρ'; 'ρ' + the leading-log QCD calculation[14] for u,d and s quarks with $\Lambda = 200$ MeV; 'ρ' + leading log + next-to-leading log QCD calculation[15] for u, d and s quarks with $\Lambda = 200$ MeV; and a quark model calculation for c quarks.
(b) $\langle Q^2 \rangle$ - x correlation for PLUTO data.

detector simulation and analysis cuts. Then the numbers of Monte Carlo events as a function of x are compared to the data and an improved approximation for F_2^γ obtained. It is desirable to iterate this procedure because of the rather loose connection between measured and actual x[12].

Now I will use the published results from PLUTO[11] to address the question: In the high-Q^2 region are we seeing $\gamma\gamma\to\rho^0\rho^0\to X$ (VDM) or $\gamma\gamma\to q\bar{q}$?

In Figure 10 the measured total cross section for $\gamma\gamma\to X$ is shown as a function of the Q^2 of the high-Q^2 photon. The expected Q^2 dependence for $\rho^0\rho^0$ scattering, given by the ρ° propagator, is also shown. Above $Q^2 = 1$ GeV^2 the data lie far above the ρ° curve, showing that at high Q^2 the photon does not behave like a ρ°.

In Figure 11a the measured x dependence of F_2^γ for $Q^2 > 1$ GeV^2 is compared to that expected for a ρ° target. The ρ° structure function, like all hadron structure function, must fall as a function of x, going to 0 at x=1 reflecting the improbability of finding one parton carrying all of a hadron's momentum. This decrease is inconsistent with the data, which is approximately flat. Therefore the low Q^2 photon is also not behaving as a ρ°, at least not when probed by a high-Q^2 photon.

We see from these comparisons that the contribution of the ρ° component of the photon is small for $Q^2 > 1$ GeV^2. We now turn to a comparison with the calculations for $\gamma\gamma\to q\bar{q}$.

Ignoring gluons, we can calculate F_2^γ for $\gamma\gamma\to q\bar{q}$ exactly in QED[13]. When the quark mass m_q is negligible we get

$$F_2^{\gamma,q\bar{q}} = \frac{3\alpha}{\pi} \sum e_i^4 \left\{ x[x^2+(1-x)^2] \ln \frac{W^2}{m_q^2} - x + 8x^2(1-x) \right\}$$

For the charmed quark, the quark mass is not negligible and the exact form[13] should be used. The results for three different Q^2 are shown in Figure 12. The strange appearance of these curves is due to the charm threshold, which moves to higher x for higher Q^2. It is clear that it will be important to understand the threshold region, which might be modified from this $\gamma\gamma\to q\bar{q}$ calculation by final state interactions. At the high-x end, the curves in Figure 12 have been terminated at the point W=1GeV, which is the usual experimental cut, and is also a value below which it does not make much sense to talk about free quarks and/or QCD. This means that the very high x region becomes inaccessible both experimentally and theoretically. In this quark model calculation I have used masses of 300 MeV for the u, d and s quarks and 1500 MeV for the c quark. The calculation

is quite sensitive to the quark masses, which is an indication that we are not in a kinematical region where the calculation is valid.

In QCD calculations, the effect of gluons is taken into account. In the leading-log calculation, all gluons emitted and not re-absorbed are included. The calculation is to all orders in α_s, but by definition includes only the leading-log terms, i.e. those terms which contain a factor $\ln Q^2$. Thus this approximation neglects the $-x+8x^2(1-x)$ term we obtained in the quark model calculation, and the argument of the logarithm, which was W^2/m_q^2, reflecting the kinematic boundary $p_t^{max} = W/2$, must be replaced by $\ln Q^2/\Lambda^2$. This loss of information is somewhat corrected in the

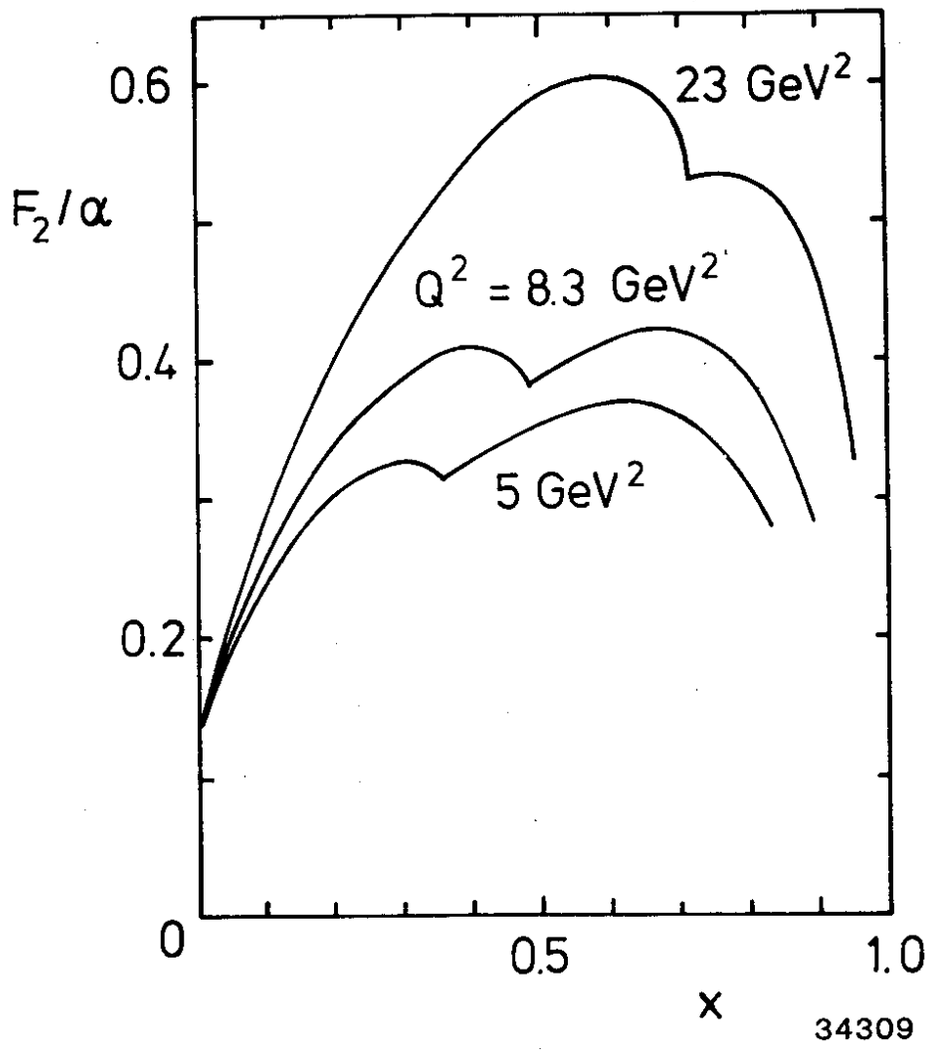

Figure 12. Photon structure function for three different Q^2 values calculated in quark model using exact QED formula[13] and masses of 300 MeV for the u, d and s quarks and 1500 MeV for the c quark. A term 0.1(1-x) has been added for the expected contribution from the ρ part of the photon.

next-to-leading-log calculations. There are various approximations made in the various next-to-leading-log calculations. Three results are compared to the leading-log calculation in Figure 13. In Figure 11a, the leading-log and one of the next-to-leading-log calculations (with Λ=200 MeV) are compared to the PLUTO data. Within the statistics, the data agrees as well with the quark model as with QCD.

A theoretically more important test is whether F_2^γ at fixed x increases with $\ln Q^2$ as expected. The PLUTO group has combined their data between x=0.2 and x=0.8 to give the Q^2 dependence in three bins from Q^2=0.5 to 15 GeV^2. Within the rather large statistical errors, the data shown in Figure 14 agrees well with the expectation. We need more statistics in order to use smaller x bins and a larger Q^2 range. I can take a tentative look at this by combining the PLUTO data at $\langle Q^2\rangle$=5GeV^2 with preliminary data from CELLO[16] at $\langle Q^2\rangle$=8.3 GeV^2 and preliminary data from JADE[17] at $\langle Q^2\rangle$=23 GeV^2 to plot $F_2^\gamma(x,\langle Q^2\rangle)$ for 5 bins in x and 3 values of $\langle Q^2\rangle$. The result, shown in Figure 15, must be taken cautiously because each experiment, which I have plotted as though $Q^2=\langle Q^2\rangle$, actually covers a wide range of Q^2.

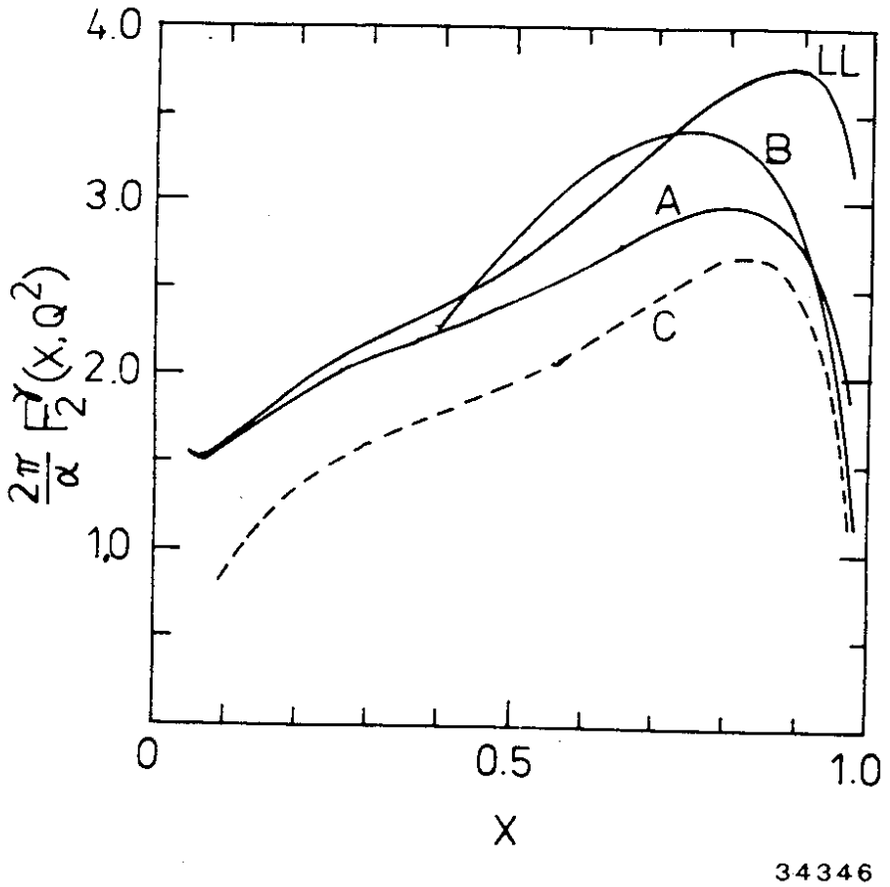

Figure 13. Photon struction function as calculated with QCD in leading log approximation (LL) and three calculations (A,B,C) in leading + next-to-leading log approximation. The plot is taken from W.Frazer, Proc. of 4th Int. Coll. on Photon-Photon Interactions, Paris, 1981.

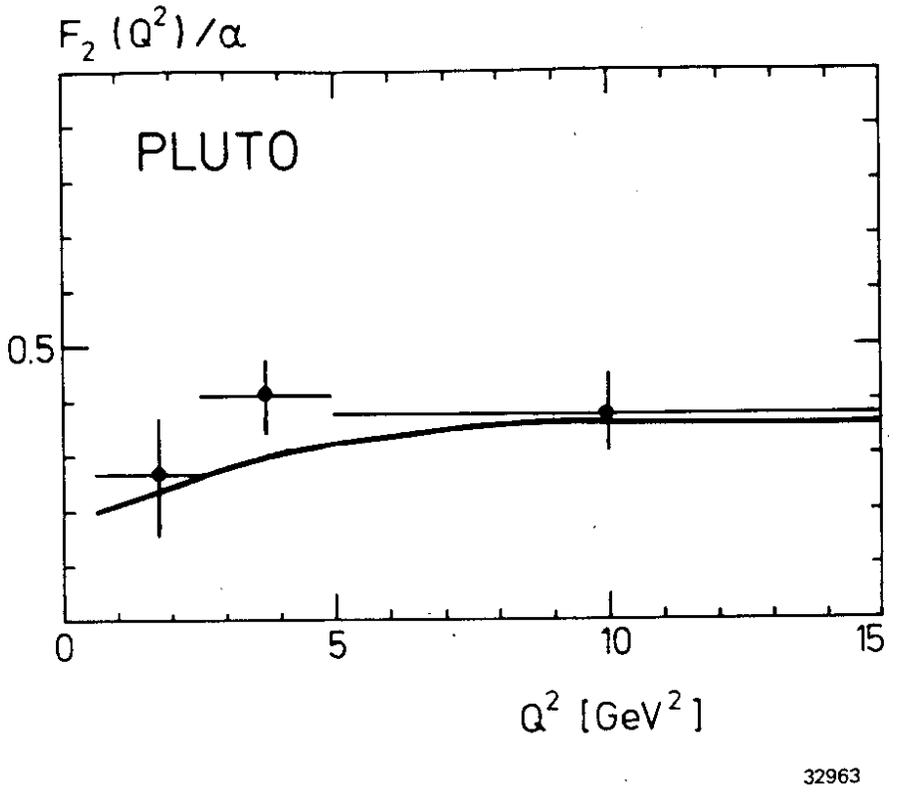

Figure 14. PLUTO photon structure function as a function of Q^2 averaged over $0.2 < x < 0.8$. The curve shows the QCD prediction in the leading-log approximation with $\Lambda = 300$ MeV.

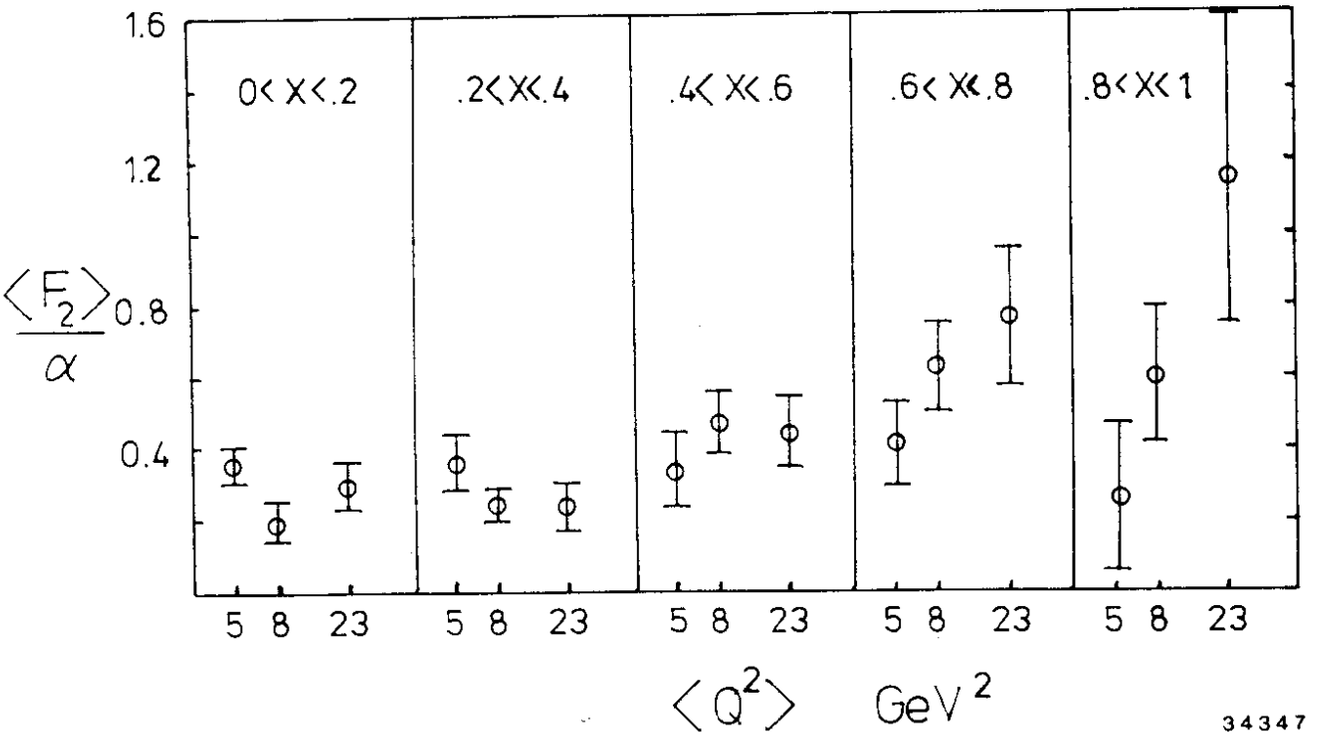

Figure 15. Q^2 dependence at fixed x of photon structure function. The data for each experiment are plotted at the average Q^2 for that experiment: PLUTO at $\langle Q^2 \rangle = 5$ GeV^2, CELLO (preliminary) at $\langle Q^2 \rangle = 8.3$ GeV^2, and JADE (preliminary) at $\langle Q^2 \rangle = 23$ GeV^2.

This is especially a problem in the region of thresholds, e.g. the bin $0.8<x<1.0$ where the cut $W > 1$ GeV is important, and the bins $0.2<x<0.4$ and $0.4<x<0.6$, which are affected by the charm threshold. One must also keep in mind that the measurement of F_2^γ is difficult, so that we should take seriously the "preliminary" for the CELLO and JADE data. Nevertheless, I have chosen to make and show such a plot to emphasize the importance of looking at the Q^2 dependence, and to suggest that cooperation between experiments in combining their data may be necessary to achieve a statistically significant result. In another year or two I hope to have such a plot with more data and without labels of "preliminary", so that we can make a serious comparison to theory.

The approximations inherent in the QCD calculations mean that measurements of the x-dependence of the structure function will test the calculation techniques more than the basic theory itself. (Testing the technique is important -- we seem to be stuck with QCD and we had better learn to calculate with it!) On the other hand, the growth of F_2^γ at fixed x is an inescapable result of the theory, and failure to see this would be a major result and a serious blow to QCD itself.

RESONANCES

Resonance production in $\gamma\gamma$ collisions has been studied in the low Q^2 region, mostly without requiring the detection of a scattered electron. The resonance is identified by detecting its decay products in the central detector. An event of the type $\gamma\gamma \to f^\circ \to \pi^+\pi^-$ is shown in our "typical" detector in Figure 16. The event is identified as a $\gamma\gamma$ event by the characteristic $\left|\sum \vec{p}_t\right| \sim 0$ and $E_{vis} \ll 2\, E_{beam}$.

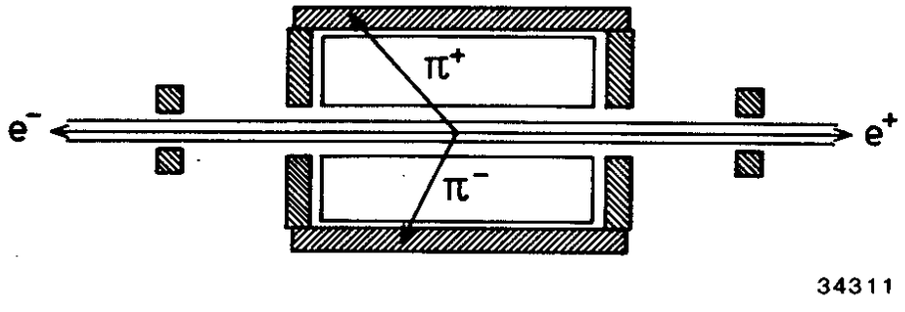

Figure 16. $\gamma\gamma \to f^\circ \to \pi^+\pi^-$ in typical detector.

The cross section for resonance production is

$$\sigma_{\gamma\gamma\to R} = 8\pi(2J+1)\ \frac{\Gamma_{\gamma\gamma}\,\Gamma}{(W_{\gamma\gamma}^2-m_R^2)^2 + \Gamma^2 m_R^2}$$

where $\Gamma_{\gamma\gamma}$ is the partial width of the resonance to $\gamma\gamma$, Γ is its total width, J its spin, and m_R its mass. It is $\Gamma_{\gamma\gamma}$ which is usually quoted, rather than $\sigma_{\gamma\gamma\to R}$.

The $\Gamma_{\gamma\gamma}$ for $q\bar{q}$ mesons can be absolutely predicted (reliably for the π^0, less so for heavier mesons). Relations between the $\Gamma_{\gamma\gamma}$ for mesons within the same $q\bar{q}$ nonet can be obtained using SU(3) invariance[18]. With these predictions, we can test the assignment of a meson to a $q\bar{q}$ nonet. Large deviations from the $q\bar{q}$ expectation may signal that the meson is actually something else. For example, $\Gamma_{\gamma\gamma}$ for a gluonium state is naively expected to be much smaller than for a $q\bar{q}$ state, since photons cannot couple directly to gluons, but must do so through an intermediate $q\bar{q}$ state, as shown in Figure 17. Therefore it is important to measure $\Gamma_{\gamma\gamma}$ for gluonium candidates. This is a case where a small upper limit is a positive result, but a larger result may be inconclusive, due to uncertainties in QCD calculations of $gg\to\gamma\gamma$.

The resonances that can be produced by two photons have even charge conjugation and spin-parity $J^P = 0^+, 0^-, 2^+, 2^-, 3^+$, etc.. Note that spin 1 is missing from the list. Two real photons are forbidden to couple to a spin 1 state by Yang's theorem[19], and since we are dealing in $\gamma\gamma$ collisions with almost-real photons, the production of spin 1 is strongly suppressed. (This might be put to good use, for example to test the controversial spin 1 assignment of the E(1420).) In the following I will discuss the $q\bar{q}$ nonets for which measurements are available: $J^P = 0^-, 2^+$, and 0^+, and then a collection of unidentified states.

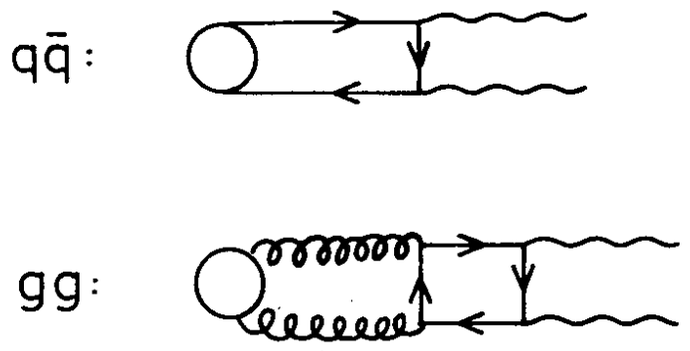

Figure 17. Diagram for the decay into two photons of a $q\bar{q}$ state and a gluonium state.

0^{-+} nonet

Table 1: 0^{-+} Nonet

0^{-+}	Predicted	Measured $\Gamma_{\gamma\gamma}$	
π°	7.6 eV	7.95±0.55 eV	world average[20]
η	395 eV*	324±46 eV	Primakoff effect[21]
η'	6.0 keV*	5.8 ± 1.1 ± 1.2 keV	Mark II (SPEAR)[22]
		5.0 ± 0.5 ± 0.9 keV	JADE[23]
		5.4 ± 1.0 ± 0.7 keV	CELLO[24]

When two errors are quoted, the first is statistical and the second systematic.
* using ϑ=–11°

The $\gamma\gamma$ widths of the π° can be reliably calculated from the triangle anomaly graph and PCAC and a factor of 3 from color. The predicted[18] 7.6 eV is in excellent agreement with the measured 7.95±0.55 eV [20].

Calculations for the η and η' must take into account that these particles are mixtures of the $q\bar{q}$ octet and singlet states:

$$\eta = \cos\vartheta\ \eta_8 - \sin\vartheta\ \eta_1$$
$$\eta' = \sin\vartheta\ \eta_8 + \cos\vartheta\ \eta_1$$

Mass relations indicate that the mixing angle ϑ is approximately -11°, which leads to the predictions shown in Table 1. The measured $\Gamma_{\gamma\gamma}$ for the η comes from a Primakoff effect measurement[21]. The $\Gamma_{\gamma\gamma}$ of the η' has been measured by the Mark II[22], JADE[23], and CELLO[24] collaborations in the reaction $\gamma\gamma\to\eta'\to\rho^\circ\gamma$. These results are in good agreement with the predictions, as shown in Table 1.

2^{++} nonet

Predictions[25] for the $\gamma\gamma$ width of the f° range between 1 and 20 keV. The measurements are shown in Table 2 as measured in $\gamma\gamma\to f^\circ\to\pi^+\pi^-$ or $\pi^\circ\pi^\circ$. The rather large systematic errors and the spread between the different experiments are due to the fact that the f° as produced in $\gamma\gamma$ collisions looks funny, and the different groups have chosen different ways of dealing with the problem. I think it is safe to say that no group is completely happy with their f° signal, but when they are considered together a pattern emerges: the f° seen in $\gamma\gamma$ collisions has a lower mass and a larger width than the standard[20] f° seen in hadronic collisions. The apparent differences to the standard values are summarized in Table 3.

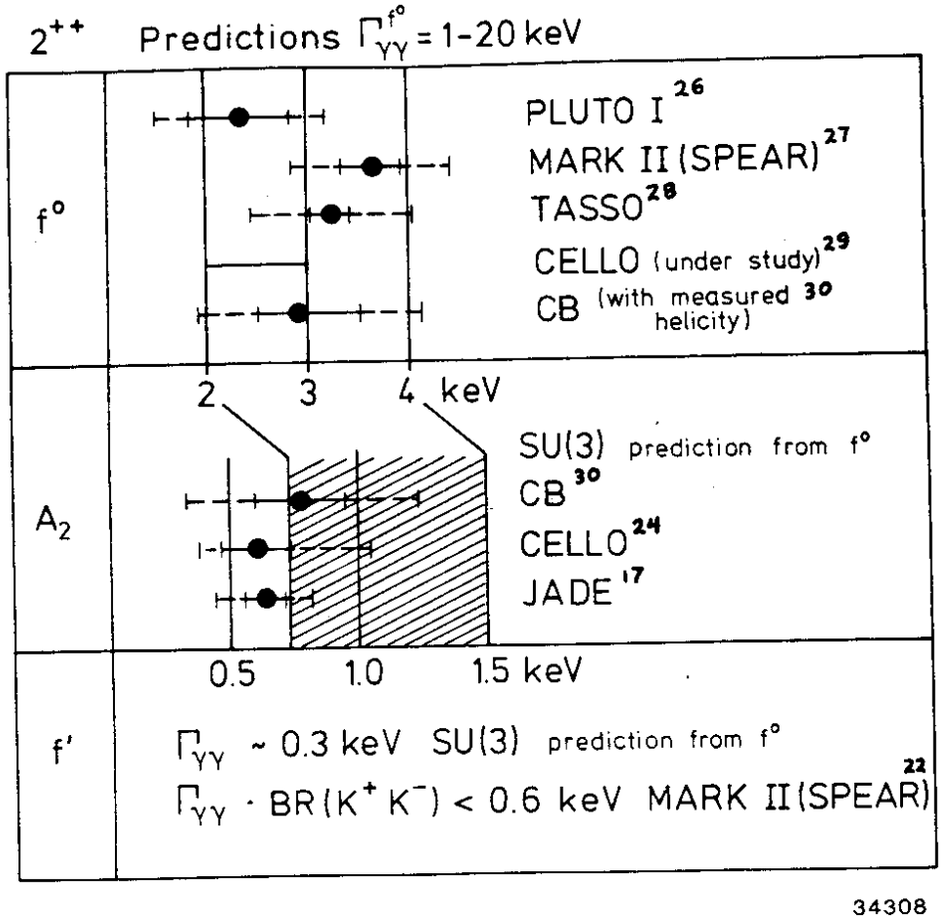

Table 2: 2^{++} nonet. The solid lines indicate the statistical error, the dotted lines the systematic error added linearly. The first four measurements for the f° use the assumption that it is produced in a helicity 2 state. The Crystal Ball result uses their measured mixture of helicities.

Experiment	Mass shift	Width shift
TASSO[28]	− 33 ± 7 MeV	+ 67 ± 21 MeV
Mark II[27]	"bad fit to standard f°"	
CELLO (prel.)[29]	− 60 ± 7 MeV	+ 20 ± 20 MeV
Crystal Ball[30]	− 35 ± 14 ± 25 MeV	+ 70 ± 38 MeV

Table 3: Apparent shifts of f° mass and width in $\gamma\gamma \to$ f° as determined in fits allowing no interference or other resonances.

The analysis is complicated by the presence of backgrounds. The QED $\gamma\gamma \to e^+e^-$ and $\gamma\gamma \to \mu^+\mu^-$ contribution is large but can be reliably calculated[31]. Some groups have partially removed it using particle identification. The Crystal Ball $\pi^\circ\pi^\circ$ data is free of this background. The $\pi\pi$ continuum is more troublesome because it cannot be calculated. We are at an energy too high to use the Born term which assumes point-like coupling of the pion to the photon, and too low to use QCD calculations. An additional problem is the detection efficiency, which drops sharply for some experiments just below the f° mass (TASSO,CB).

A possible explanation of the mass shift is interference between the f° and the $\pi\pi$ continuum. The Mark II group has shown[27] (Figure 18) that interference with the Born term can explain their data, which however has little sensitivity above the f° mass due to the low photon-photon flux in this mass range at SPEAR ($E_{beam} \lesssim 3$ GeV). However the TASSO[28] and PLUTO[32] collaborations have shown that this Born term gives far too many events above the f° mass. On the other hand the Born term gives about a factor of two too few events on the low mass side to explain the DCI[33] data. In any case, the Born term is zero for $\pi^\circ\pi^\circ$, and therefore can't explain the Crystal Ball data[30]. As a last blow, any theorist would say that the Born term can't be right. In order to decide whether interference is the right explanation, we must first come to grips with the continuum itself. Work on this is in progress in the CELLO collaboration[29] using a phenomenological "unitarized" Born term[34].

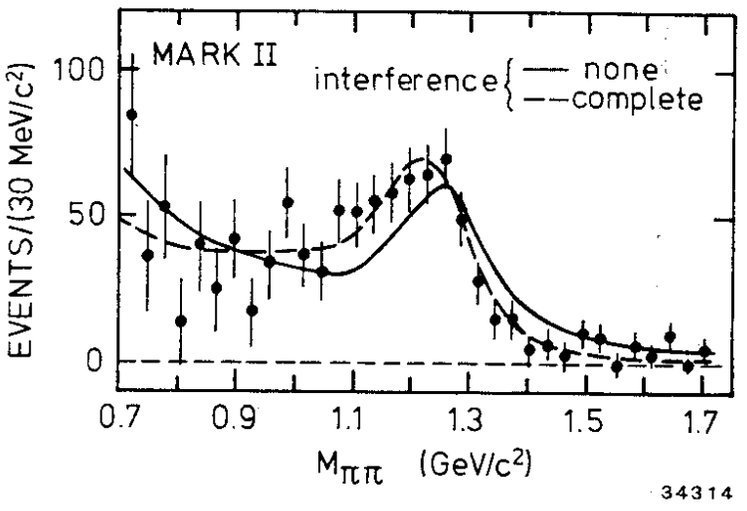

Figure 18. Mark II $\gamma\gamma \to \pi^+\pi^-$ compared to Born term + f° with and without interference.

Another possible explanation is that the f° seen in $\gamma\gamma$ collisions is not the same as the f° produced in hadron collisions. It has been suggested[35] that mixing with a nearby 2^{++} gluonium state means that the f° produced in hadronic reactions is partly $q\bar{q}$ and partly gg. In $\gamma\gamma$ collisions the $q\bar{q}$ part would be more strongly excited than the gg part which lacks a direct coupling to photons. This could change the mass and width, and the decay branching ratios would also be affected. Therefore it is important to compare the branching ratios for f°'s produced in $\gamma\gamma$ and hadron collisions. Likely to be affected by a gluonium mixture are f°→KK and f°→$\eta\eta$. So far we have only upper limits:

$$\frac{BR(f^{\gamma\gamma}\to K^+K^-)}{BR(f^{had}\to K^+K^-)} < 7 \qquad \text{Mark II}^{22}$$

and

$$\frac{BR(f^{had}\to \eta\eta)}{BR(f^{had}\to \pi\pi)} < 2\% \quad \text{vs.} \quad \frac{BR(f^{\gamma\gamma}\to \eta\eta)}{BR(f^{\gamma\gamma}\to \pi\pi)} < 5\% \qquad \text{CB}^{30}$$

A solution of the f° problem requires better understanding of the $\pi^+\pi^-$ as well as the $\pi^\circ\pi^\circ$ continuum, which means extending measurements well below the f° mass, and in addition better measurements in other channels such as KK and $\eta\eta$.

Continuing on in the 2^{++} nonet, we come to the A_2, whose $\gamma\gamma$ width has been measured by the Crystal Ball[30] with the decay channel $\eta\pi^\circ$, and by JADE[17] and CELLO[24] in the decay $\rho\pi$. The measurements agree well with each other, as shown in Table 2. The SU(3) translation of the f°'s 2-4 keV into a prediction for the A_2 is also shown in the figure. Given the difficulties with the f°, it is not surprising that the measurements tend to lie on the low side.

The third neutral member of the 2^{++} nonet, the f'(1515) which decays primarily into KK, may be strongly affected[36] by interference with the KK channels of the f° and A_2. At present only an upper limit is available:

$$\Gamma_{\gamma\gamma}^{f'} \cdot BR(f'\to K^+K^-) < 0.6 \text{ keV} \qquad \text{Mark II}^{22}$$

which was obtained neglecting interference. Further work on the KK spectrum is in progress.

0^{++} nonet

Table 4: 0^{++} Nonet

0^{++}	(Predictions are ~ 20 M^3)	
? $\varepsilon(700)$	$\Gamma_{\gamma\gamma}$ ~ 40 keV ?	DCI[33]
$\varepsilon(1425)$	$\Gamma_{\gamma\gamma}$ * BR($\pi^+\pi^-$) < 1.5 keV	TASSO[28]
S*(980)	$\Gamma_{\gamma\gamma}$ * BR ($\pi\pi$) < 0.8 keV	CB[30]
$\delta(980)$		

The 0^{++} nonet is not very well understood. Candidates for the neutral members include an $\varepsilon(700)$, an $\varepsilon(1300$ or $1425)$, the S*(980) and the $\delta(980)$. A fit to the DCI $\gamma\gamma\to\pi^+\pi^-$ data using the unitarized Born term and an $\varepsilon(700)$ required a $\gamma\gamma$ width for the $\varepsilon(700)$ of about 40 KeV. However, since the ε could not be seen as a peak in this experiment, whose data stops at about 700 MeV, the presence of the ε is inferred only from the excess of the data over the unitarized Born term. A recent phase shift analysis[37] of $\pi^\circ\pi^\circ$ data prefers a different parameterization of the ε from what was used in the DCI fit. Again we come to the need for high statistics $\gamma\gamma\to\pi\pi$ data extending from just above threshold to well above the resonance region so that we have enough constraints on the continuum in order to be able to reliably extract the resonances from it.

The heavier ε and the S* have rather small $\gamma\gamma$ widths, as shown by the upper limits in Table 4. These limits are considerably smaller than the $\sim 20M^3$ (M in GeV) expected[38] in most theoretical estimates, but consistent with a single-quark-exchange calculation[39] which predicts 0 - 0.4 keV for 0^{++} mesons.

Since there is speculation that the S* and δ are $q\bar{q}q\bar{q}$ states, it would be interesting to have measurements of the $\gamma\gamma$ widths of the $\varepsilon(1425)$, S* and δ to see if they are consistent with the SU(3) relations for mesons within a nonet. However, since their $\gamma\gamma$ widths are apparently small, this will be difficult.

Other states

We now turn to states which have not yet found a place in our scheme for understanding meson resonances. The first of these may or may not be a resonance. In 1980 the TASSO collaboration observed[42] a cross section for $\gamma\gamma\to\rho^0\rho^0$ which was much larger than expected from VDM calculations. This large cross section, which has since been seen by other experiments[43], led to speculations that some new resonance was being excited, either a new $q\bar{q}$ state or perhaps a $q\bar{q}q\bar{q}$ or gluonium state.

Table 5: Other States

	J^P	Mass (GeV)	Width (GeV)	$\Gamma_{\gamma\gamma}$	
$\rho^0\rho^0$	$0^+,2^+$	1.2 - 1.7	very broad		TASSO[40]
ι	0^-	1440 ± 15	55 ± 20	$\Gamma_{\gamma\gamma}$ * BR(KKπ) < 8 keV	Mark II[22]
				$\Gamma_{\gamma\gamma}$ * BR($\rho^0\rho^0$) < 1.0 keV	TASSO[40]
θ	2^+	1640 ± 50	220 ± 90	$\Gamma_{\gamma\gamma}$ * BR($\eta\eta$) < 5 keV	CB[41]
				$\Gamma_{\gamma\gamma}$ * BR($\rho^0\rho^0$) < 1.2 keV	TASSO[40]

A preliminary new cross section determination from TASSO[40] extends the measurement below the nominal $\rho^0\rho^0$ threshold at 1.5 GeV and shows that $\rho^0\rho^0$ production remains large down to 1.2 GeV. The peculiarity of this behaviour is demonstrated in Figure 19 where the measured cross section is compared to a calculation of $\rho^0\rho^0$ phase space. The TASSO collaboration has also performed a spin-parity analysis.

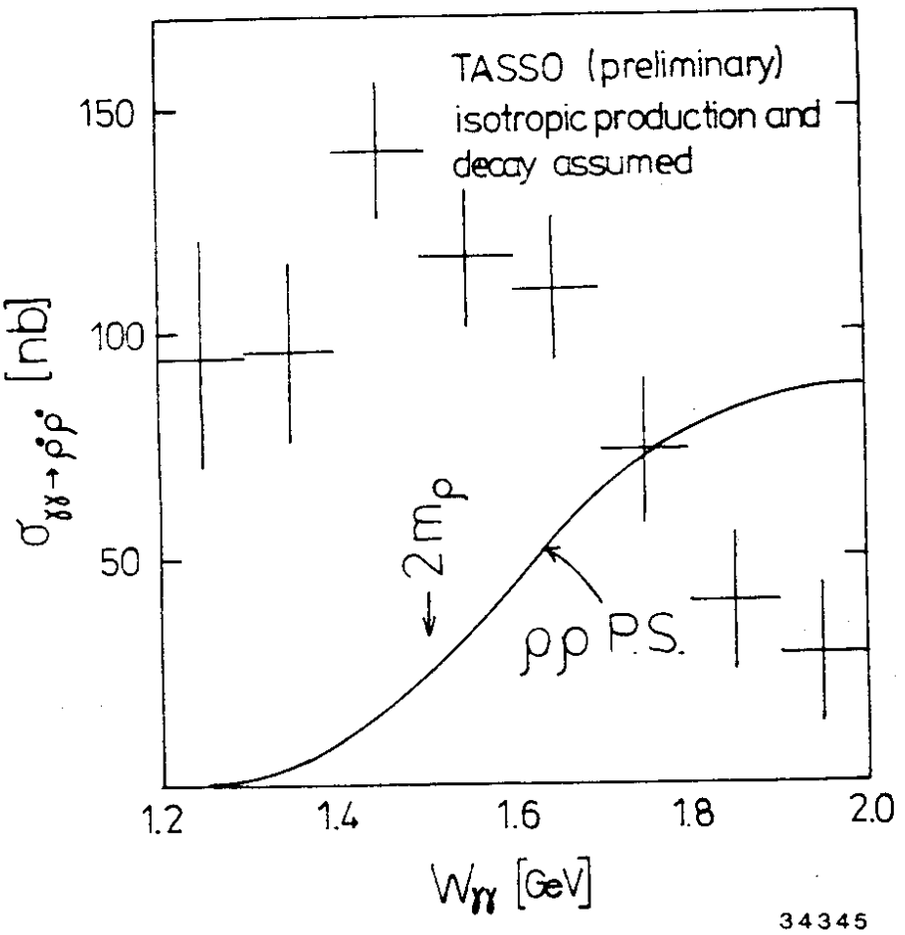

Figure 19. preliminary TASSO $\gamma\gamma\to\rho^0\rho^0$ total cross section assuming isotropic production and decay of the $\rho^0\rho^0$ system. The detection efficiency changes by up to a factor of 2 for the various possible J^{PC} states.

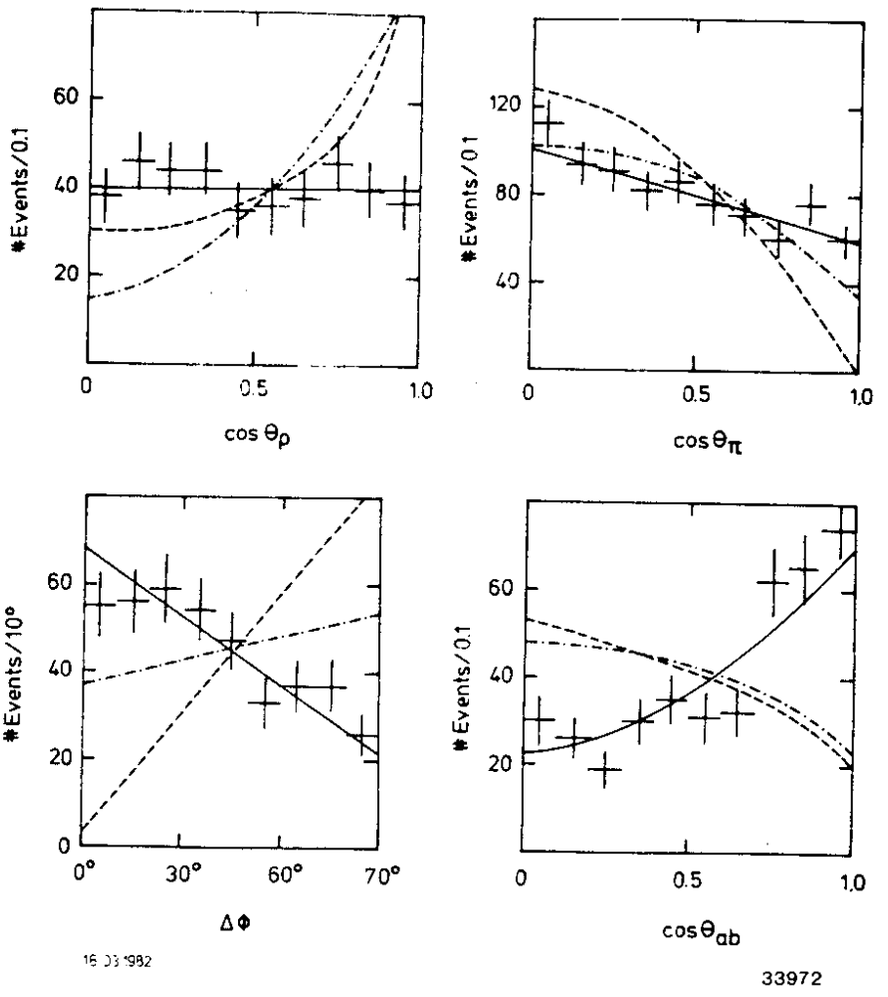

Figure 20. Observed angular distributions for TASSO $\gamma\gamma \to \rho^0\rho^0$ data compared to Monte Carlo calculations including the effects of the TASSO acceptance for $J^{PC} = 0^{-+}$ (dashed line) and 2^{-+} (dot-dashed line) and for the best fit (full line). The data are in the mass range $1.4 < M_{4\pi} < 1.6$ GeV. To enter the plots events had to have both $\pi^+\pi^-$ masses within 150 MeV of the nominal ρ mass for at least one $\pi^+\pi^-$ - $\pi^+\pi^-$ combination. If both $\pi^+\pi^-$ - $\pi^+\pi^-$ combinations are within this cut, they both appear in the plots.

a) the ρ production angle ϑ_ρ defined in the $\gamma\gamma$ CM system with the z-axis along the beam axis.

b) the ρ decay angle ϑ_π defined as the polar angle of the π^+ of each ρ° in the ρ helicity frame.

c) the angle $\Delta\varphi$ between the decay planes of the 2 ρ°'s

d) the cosine of the three-dimensional opening angle ϑ_{ab} between the two π^+ directions, each defined in its respective ρ° helicity frame.

They find that within their acceptance it is not possible to reliably distinguish between isotropic production and decay of $\rho^0\rho^0$ and $\rho^0\rho^0$ production through a $J^{PC} = 0^{++}$ or 2^{++} state. All three possibilities agree with the data. However $J^{PC} = 0^{-+}$ and 2^{-+} have distinct characteristics which differ strongly fom the data, as shown in Figure 20. We are left with the possibility that the observed $\gamma\gamma\to\rho^0\rho^0$ is a threshold effect, or is perhaps due to a broad resonance with $J^{PC} = 0^{++}$ or 2^{++} and a mass $\lesssim 1.2$ GeV. Alternatively, a recent calculation[44] suggests that the effect can be explained by VDM after all. It would be interesting to have information on other vector meson channels $\gamma\gamma\to VV$, and to try for better acceptance in order to distinguish between $J^{PC} = 0^{++}$ and 2^{++}.

In the meantime two new states found in radiative ψ decay have excited much talk about gluonium. This makes them interesting to two-photon physicists because of the potential importance of $\Gamma_{\gamma\gamma}$ in distinguishing $q\bar{q}$ from gluonium states. The first of these two states is the $\iota(1440)$ seen in $\psi \to \gamma$ KKπ by the Mark II[45] and Crystal Ball[46] collaborations. The Mark II group using their SPEAR data[22] for $\gamma\gamma\to$KKπ has set an upper limit for the $\gamma\gamma$ width of this state of

$$\Gamma_{\gamma\gamma}^{\iota} \cdot BR(\iota\to K\bar{K}\pi) < 8 \text{ keV}.$$

This is not yet small enough to be helpful, but data at higher beam energies, where the $\gamma\gamma$ flux in this mass range is substantially higher, should allow a better measurement. The TASSO collaboration, in showing that their $\gamma\gamma\to\rho^0\rho^0$ data is not due to this state, has set a preliminary upper limit of

$$\Gamma_{\gamma\gamma}^{\iota} \cdot BR(\iota\to\rho^0\rho^0) < 1.0 \text{ keV} \quad (95\%\text{CL})$$

However the branching ratio of the decay $\iota\to\rho^0\rho^0$ is not known.

A second state, the $\Theta(1640)$ was observed[47] by the Crystal Ball collaboration in $\psi \to \gamma\,\eta\eta$. Using their $\gamma\gamma\to\eta\eta$ data, they have set an upper limit of

$$\Gamma_{\gamma\gamma}^{\Theta} \cdot BR(\Theta\to\eta\eta) < 5 \text{ keV} \quad (95\% \text{ CL})$$

The TASSO collaboration has a preliminary upper limit for this state using their $\gamma\gamma\to\rho^0\rho^0$ data and the measured Crystal Ball parameters for the Θ of

$$\Gamma_{\gamma\gamma}^{\Theta} \cdot BR(\Theta\to\rho^0\rho^0) < 1.2 \text{ keV} \ (95\% \text{ CL})$$

Preliminary Mark II results[48] on $\psi \to \gamma\,\rho^0\rho^0$ have shown a large peak at the same mass and width as the Θ, but they have not yet performed a spin-parity analysis. If this is indeed the Θ, the $\rho^0\rho^0$ represents a large decay mode, and the TASSO upper limit begins to look rather small for a $q\bar{q}$ state.

CONCLUSION

In conclusion I would like to say that two-photon physics is thriving at e^+e^- storage rings, doing physics ranging from the study of resonances to tests of QCD. There is much left to do, and there are data available to do it with.

The first results on the photon structure function have been very successful in showing that the $\gamma\gamma \to q\bar{q}$ process stands out clearly against VDM background. More statistics will allow tests of the QCD expectation for the Q^2 dependence at fixed x. Measurement of the total hadronic energy is crucial for determination of the photon structure function. Perhaps a calorimetric experiment can do better than one which emphasizes charged particles. The Monte Carlo model dependence in the correction for the unseen energy should be checked. On the theory side, work needs to be done on dealing as accurately as possible with the known kinematic effects within the framework of QCD calculations.

In the resonance region we have several open questions. The f° and the 0^{++} nonet are both puzzles which call for a careful study of the $\pi\pi$ background. Mixing of gluonium with known hadrons can be tested for by checking the resonance shapes and branching ratios of these hadrons when produced in $\gamma\gamma$ collisions. In addition the measurement of the $\gamma\gamma$ width is an important test for gluonium candidates. Two photon collisions have given us a puzzling effect in the $\rho^0\rho^0$ channel, and we should always be on the lookout for other surprises.

ACKNOWLEDGEMENTS

I would like to thank the Bonn group of TASSO, where I learned all I know about two photon physics, for two years of work together in a very pleasant atmosphere. In addition, I thank Walter Hillen, Hermann Kolanoski and Kay Königsmann for particularly helpful comments on this paper, and John Field and Jan Olsson for discussions of the CELLO and JADE data.

REFERENCES

[1] The first no-tag two-photon physics was done by the Mark II: G.S.Abrams et.al., Phys.Rev.Lett.43 (1979) 477.

[2] (PLUTO) Ch.Berger et.al., Phys.Lett.89B (1981) 287.
(TASSO) W.Hillen, Ph.D. Thesis, BONN-IR-81-7 (1980) and E.Hilger, Proc. Int. Workshop on $\gamma\gamma$ Collisions, Amiens, 1980, Published by Springer as Lecture Notes in Physics 134 (1980).

[3] (TASSO) N.Wermes, Ph.D. Thesis, BONN-IR-82- (1982).

[4] The 10/3 expected for the Han-Nambu integrally charged quark model can be affected by the Q^2 of the photons to an extent that it is indistinguishable from the fractionally charged quark model: T. Jayaraman et.al. Madras Univ. Preprint MUTP-82/3 (1982).

[5] S.Berman et.al., Phys.Rev. D4 (1971) 3388; S.Brodsky et.al., Phys.Rev. D5 (1979) 1418 and PRL 41 (1978) 527.

[6] (TASSO) R. Brandelik et.al., Phys.Lett. 107B (1981) 290.
(JADE) W. Bartel et.al., Phys.Lett. 107B (1981) 163.

[7] P.H.Damgaard, Cornell Lab. of Nucl. Studies Preprint CLNS-81/519 (Dec. 1981).

[8] (TASSO) R.Brandelik et.al., Phys.Lett. 108B (1982) 67; and new preliminary results from JADE and TASSO presented at the Rencontre de Moriond, Les Arcs, France in March 1982 by H.Kolanoski and J.Olsson.

[9] The equivalent photon approximation is no longer used by most experimental groups. Exact calculations are available and have been put into useful form in J. Field, Nucl.Phys. B168 (1980) 477 and Erratum B176 (1980) 545, and Ch.Berger and J.Field, Nucl.Phys.B187 (1981) 585.

[10] It is a convention from eN scattering that a kinematic factor which suppresses longitudinal photons is removed from L^{LT} and absorbed into σ^{LT}. (See e.g. page 469 in M. Perl's book High Energy Hadron Interactions published by John Wiley and Sons in 1974.) Keeping this change of definition in mind, we see that the fact that $\varepsilon = L^{LT}/ L^{TT}$ is nearly 1 at low Q^2 does not mean that we really have nearly as many longitudinal as transverse photons.

[11] (PLUTO) Ch.Berger et.al., Phys.Lett. 107B (1981) 168.

[12] Most groups use an x vs. x_{meas} matrix to "unfold" their x_{meas} distribution into an x distribution. However some dependence of the input F_2^γ might still remain.

[13] The exact result for F_2^γ can be obtained using the formulas for σ^{TT} and $\sigma^{ST} = \sigma^{LT}$ on page 275 of V.M.Budnev et.al., Physics Reports 15 no.4 (1975) 181.

[14] W.Frazer and J.Gunion, Phys.Rev.D20 (1979) 147.

[15] A.J.Buras and D.W.Luke, unpublished, shown in Ref. 11.

[16] (CELLO) J.Haissinski, Rencontre de Moriond, Les Arcs, France, March 1982 and Orsay Preprint LAL 82/11.

[17] (JADE) J.Olsson, Rencontre de Moriond, Les Arcs, France, March 1982.

[18] reviewed in F.Gilman, Proc. Int. Conf. on Two Photon Interactions, Lake Tahoe, Calif., 1979.

[19] C.N.Yang, Phys. Rev. 77 (1950) 242.

[20] summarized in Particle Data Group, "Review of Particle Properties", Rev.Mod.Phys. 52, No.2 (1980).

[21] A.Browman et.al., PRL 32 (1974) 1067.

[22] (Mark II) G.S.Abrams et.al., Phys.Rev.Lett.43 (1979) 477,
P.Jenni et.al. sub. to Phys. Rev. D, June 1982, SLAC-PUB-2758, LBL-10226, June 1981.

[23] (JADE) W.Bartel et.al., DESY 82-007 (1982).

[24] (CELLO) H.J.Behrend et.al.,DESY 82-008 (1982).

[25] $\Gamma_{\gamma\gamma}^{f}$ predictions are shown in E.Hilger, Proc. 4th Int. Coll. on Photon-Photon Interactions, Paris, 1981.

[26] (PLUTO) Ch.Berger et.al., Phys.Lett. 94B (1980) 254.

[27] (Mark II) A.Roussarie. SLAC-PUB-2599 and XXth Int. Conf. on High Energy Physics, Madison, Wisconsin, 1980.
A.Roussarie et.al., Phys.Lett. 105B (1981) 304.

[28] (TASSO) R.Brandelik et.al., Z.Physik C 10 (1981) 117.

[29] (CELLO) J.Field, private communication.

[30] (CB) C.Edwards et.al. Phys.Lett. 110B (1982) 82.

[31] Monte Carlo calculation: (program of J.A.M.Vermaseren):
R.Bhattacharya,J.Smith,and G.Grammer,Jr.,Phys.Rev.D15 (1977)3267.
measurements: (Mark II) A.Roussarie SLAC-PUB-2599 and Proc. XXth Int. Conf. on High Energy Physics, Madison, Wisconsin, 1980.
(Mark J) B.Adeva et.al., MIT Tech. Rep. 112 (1982).

[32] (PLUTO) Ch. Berger et.al., DESY 82-004 (1982). sub. to Nucl.Phys.B

[33] (DCI) A. Falvard et.al., contributed paper no.48, Int. Symp. on Lepton-Photon Interactions, Bonn, 1981.; Proc. Gamma Gamma Physics, Amiens, Dec. 1981; Phys.Lett. 96B (1980) 402.

[34] G. Mennessier, contributed paper no.42, Int. Symp. on Lepton-Photon Interactions, Bonn, 1981 and Montpellier Preprint PM/81/6 (1981).

[35] J.Rosner, Phys.Rev.D24 (1981) 1347.

[36] D.Faimann et.al., Phys.Lett. 59B (1975) 269.

[37] N.N.Biswas or V.P.Kenney et.al. PRL 47 (1981) 1378.

[38] summarized in M.Greco, Proc. Int. Workshop on $\gamma\gamma$ Collisions, Amiens, 1980.

[39] J.Babcock and J.Rosner, Phys.Rev.D (1976) 1286.

[40] (TASSO) private communication and H. Kolanoski, Proc. of Rencontre de Moriond, Les Arcs, France, March 1982.

[41] (CB) private communication

[42] (TASSO) R.Brandelik et.al., Phys.Lett. 97B (1980) 448.

[43] (Mark II) D.L.Burke et.al., Phys.Lett. 103B (1981) 153.
(CELLO) contibuted paper to Int. Conf. on High Energy Physics, Lisbon, 1981.

[44] G.Alexander and U.Maor, Tel Aviv Preprint TAUP 1024-82.

[45] (Mark II) D.L.Scharre et.al., Phys.Lett. 97B (1980) 329.

[46] (CB) D.L.Scharre, Proc. Int. Symp. on Lepton-Photon Interactions, Bonn, 1981; C.Edwards et.al., SLAC-PUB-2896 (1982) sub. to PRL.

[47] (CB) C.Edwards et.al., PRL 48 (1982) 458.

[48] (Mark II) SLAC-PUB-2941, sub. to Phys.Lett.